Inorg. Chem. **2002**, *41*, 2879–2885

Synthesis, Structural Trends, and Physical and Electronic Properties of the Reduced Molybdenum Oxides $R_4Mo_4O_{11}$ (R = Nd–Tm and Y) Containing Infinite Chains of Trans-Edge-Shared Octahedral Clusters

P. Gall,[†] N. Barrier,[‡] R. Gautier,[§] and P. Gougeon*[,‡]

Laboratoire de Chimie du Solide et Inorganique Moléculaire, UMR CNRS No. 6511, Université de Rennes 1, Institut de Chimie de Rennes, Avenue du Général Leclerc, 35042 Rennes Cedex, France, Laboratoire de Chimie des Matériaux Inorganiques et de Cristallographie, 20 av des buttes de Coesmes, 35043 Rennes Cedex, France, and Département de Physicochimie UPRES 1795, Ecole Nationale Supérieure de Chimie de Rennes, Institut de Chimie de Rennes, Campus de Beaulieu, 35700 Rennes Cedex, France

Received September 25, 2001

The new compounds $R_4Mo_4O_{11}$ (R = Y, Nd, Sm–Tm) have been synthesized as crystalline powders by solid-state reaction in a sealed molybdenum crucible at 1400 °C. Single crystals suitable for X-ray structure determinations and resistivity measurements were also prepared. The $R_4Mo_4O_{11}$ compounds crystallize in the orthorhombic space group *Pbam* with four formulas per unit cell. The crystal structure of these compounds is based on infinite chains of trans-edge-shared molybdenum octahedra, which are widely separated by the rare-earth cations that are in monocapped trigonal prismatic coordination of oxygen atoms. Consequently, adjacent metallic chains do not share oxygen atoms and the shortest interchain Mo–Mo distance is greater than 7 Å. Within the infinite chains, a strong pairing between the apical Mo atoms occurs, leading to a pattern of alternating short and long distances between these atoms. Resistivity measurements on single crystals show that the $R_4Mo_4O_{11}$ compounds are small band gap semiconductors, and magnetic susceptibility studies are in agreement with the presence of R^{3+} ions. In addition, antiferromagnetic orderings have also been observed for the $R_4Mo_4O_{11}$ compounds with R = Gd–Tm below 5 K. Theoretical calculations confirm the stabilization of the structure by the distortion and agree with the resistivity and magnetic measurements.

Inroduction

Since the first report of infinite chains of trans-edge-sharing Mo_6 octahedra in $NaMo_4O_6$ by Torardi and Mc Carley in 1979,[1] four other crystallographic structure types containing similar molybdenum chains have been discovered: $Sc_{0.75}Zn_{1.25}Mo_4O_7$,[2] $Mn_{1.5}Mo_8O_{11}$,[3] MMo_8O_{10} (M = Li, Zn),[4] and $Ho_4Mo_4O_{11}$.[5] The crystal structures of these compounds differ from each other in the manner in which the infinite molybdenum octahedral chains are coupled together through the oxygen atoms to form the three-dimensional lattices. Thus, whereas the molybdenum chains are parallel in $Sc_{0.75}Zn_{1.25}Mo_4O_7$, $Mn_{1.5}Mo_8O_{11}$, and $Ho_4Mo_4O_{11}$, they are crosswise in MMo_8O_{10}. In addition, it should be mentioned that infinite trans-edge-sharing Mo_6 chains are also observed in the series of compounds $R_4Mo_{18}O_{32}$ (R = Gd−Lu, Y)[6] in which they coexist with chains of single Mo atoms similar to that encountered in MoO_2[7] and chains of planar rhomboidal Mo_4 clusters. Another important difference between the trans-edge-sharing

* Author to whom correspondence should be addressed. E-mail: Patrick.Gougeon@univ-rennes1.fr.

[†] Laboratoire de Chimie des Matériaux Inorganiques et de Cristallographie.

[‡] Université de Rennes 1, Institut de Chimie de Rennes.

[§] Ecole Nationale Supérieure de Chimie de Rennes, Institut de Chimie de Rennes.

(1) Torardi, C. C.; McCarley, R. E. *J. Am. Chem. Soc*. **1979**, *101*, 3963.
(2) McCarley, R. E. *Philos. Trans. R. Soc. London A* **1982**, *308*, 41.
(3) Carlson, C. D.; Brough, L. F.; Edwards, P. A.; McCarley, R. E. *J. Less-Common Met.* **1989**, *156*, 325.
(4) Lii, K. H.; McCarley, R. E.; Kim, S.; Jacobson, R. A. *J. Solid State Chem*. **1986**, *64*, 347.
(5) Gougeon, P.; Gall, P.; McCarley, R. E. *Acta Crystallogr*. **1991**, *C47*, 1585.
(6) (a) Gougeon, P.; Gall, P.; McCarley, R. E. *Acta Crystallogr*. **1991**, *C47*, 2026. (b) Gall, P.; Gougeon, P.; Greenblatt, M.; McCarroll, W. H.; Ramanujachary, K. V. *J. Solid State Chem*. **1997**, *134*, 45.
(7) Magneli, A.; Anderson, G.; Holmberg, B.; Kihlborg, L. *Anal. Chem.* **1952**, *24*, 1998.

10.1021/ic011000i CCC: $22.00
Published on Web 05/07/2002

Table 1. Crystallographic and Experimental Data for $R_4Mo_4O_{11}$ (R = Sm−Tm, Y)

formula	$Sm_4Mo_4O_{11}$	$Eu_4Mo_4O_{11}$	$Gd_4Mo_4O_{11}$	$Tb_4Mo_4O_{11}$	$Dy_4Mo_4O_{11}$	$Er_4Mo_4O_{11}$	$Tm_4Mo_4O_{11}$	$Y_4Mo_4O_{11}$
fw	1161.16	1167.60	1188.76	1195.44	1209.76	1228.80	1235.48	915.40
space group	*Pbam*	*Pbam*	*Pbam*	*Pbam*	*Pbam*	*Pbam*	*Pbam*	*Pbam*
a (Å)	10.8700(7)	10.8351(7)	10.7940(7)	10.7369(6)	10.7055(8)	10.6270(8)	10.5874(6)	10.6619(9)
b (Å)	16.0957(14)	16.0477(13)	15.9876(13)	15.9112(12)	15.8721(15)	15.7629(15)	15.7134(12)	15.8167(17)
c (Å)	5.7178(2)	5.7042(2)	5.6942(2)	5.6764(2)	5.6640(2)	5.6396(2)	5.6282(2)	5.6517(2)
V (Å^3)	1000.4(1)	991.8(1)	982.7(1)	969.7(1)	962.4(1)	944.7(1)	936.3(1)	953.1(1)
Z	4	4	4	4	4	4	4	4
D_{calcd} (g/cm^3)	7.71	7.82	8.03	8.19	8.35	8.64	8.76	6.38
T, °C	20	20	20	20	20	20	20	20
λ, Å	0.71073	0.71073	0.71073	0.71073	0.71073	0.71073	0.71073	0.71073
μ (cm^{-1})	279.7	297.8	315.7	338.1	359.3	402.9	427.0	291.9
R1[a] [$I > 2\sigma(I)$]	0.0236	0.0216	0.0265	0.0261	0.0340	0.0254	0.0258	0.0351
wR2[b] [$I > 2\sigma(I)$]	0.0529	0.0318	0.0557	0.0402	0.0508	0.0437	0.0370	0.0523

[a] $R1 = \sum||F_o| - |F_c||/\sum|F_o|$. [b] $wR2 = \{\sum[w(F_o^2 - F_c^2)^2]/\sum[w(F_o^2)^2]\}^{1/2}$, $w = 1/[\sigma^2(F_o^2) + (aP)^2 + bP]$ where $P = [\mathrm{Max}(F_o^2,0) + F_c^2]/3$.

Mo_6 octahedral chains present in the above different structure types is the number of electrons available for Mo−Mo bonding, often called metal-centered electrons (MCE). The MCE on which greatly depend the physical properties in these materials vary from 13 electrons per Mo_4 repeat unit in the MMo_4O_6 (M = Na, K, In) compounds to 15 in $ZnMo_8O_{10}$. Although these compounds would be good candidates to exhibit interesting physical phenomena such as charge-density wave or metal insulator transition because of the one-dimensional character of the Mo network, only KMo_4O_6 (13 e$^-$/Mo_4)[8] and $Mn_{1.5}Mo_8O_{11}$ (14.5 e$^-$/Mo_4)[3] have been the subject of physical property studies to date. Both compounds are metallic from 300 to 50 K. Below 50 K, KMo_4O_6 undergoes a metal−insulator transition while $Mn_{1.5}Mo_8O_{11}$ remains metallic down to 4.2 K. This paper deals with the synthesis, crystal growth, magnetic and electrical properties, and theoretical study of the series of compounds $R_4Mo_4O_{11}$ (R = Y, Nd, Sm−Tm) belonging to the $Ho_4Mo_4O_{11}$ structure type.

Experimental Section

Synthesis. Single-phase powder samples of the $R_4Mo_4O_{11}$ compounds were prepared from stoichiometric mixtures of MoO_3 (Strem Chemicals, 99.9%), Mo (Cime bocuze, 99.99%), and R_2O_3 (R = Nd, Sm, Eu, Gd, Dy−Tm) (Strem Chemicals, 99.999%), all in powder form. For the Tb compound, the starting rare-earth oxide was Tb_4O_7 (Strem Chemicals, 99.999%). Before use the Mo powder was heated under a hydrogen flow at 1000 °C for 6 h and the rare-earth oxides were prefired at temperatures between 700 and 1000 °C overnight and left at 600 °C before being weighed. The mixtures were pressed into pellets (ca. 5 g) and loaded into molybdenum crucibles which were previously outgassed at about 1500 °C for 15 min under a dynamic vacuum of about 10^{-5} Torr. The Mo crucibles were subsequently sealed under a low argon pressure using an arc welding system. The samples were heated at a rate of 300 °C/h to 1400 °C for 48 h and then cooled at 100 °C/h down to 1100 °C, at which point the furnace was shut down and allowed to cool to room temperature. All products were found to be single phase on the basis of their X-ray powder diffraction pattern carried out on an Inel position sensitive detector with a 0−120° 2θ aperture and Cu Kα_1 radiation. With the exception of the Nd compound, single crystals of the other rare-earth members (Y, Sm−Tm) in this series can be obtained large enough ($0.2 \times 0.2 \times 1.5$ mm^3) for single-crystal work by heating a mixture of K_2MoO_4, R_2O_3 (or Tb_4O_7), MoO_3, and Mo in a molar ratio of 1:1:1.33:1.66 (2:1:2.33:3.66 for the Tb compound) at 1700 °C over 48 h. These single crystals grew in the form of black needles with approximately rectangular cross sections. The absence of potassium in the crystals thus synthesized was checked by qualitative microanalyses using a JEOL JSM-35 CF scanning electron microscope equipped with a Tracor energy-dispersive-type X-ray spectrometer and confirmed by the single-crystal structure determinations.

Single-Crystal Structure Determinations. The first member of the $R_4Mo_4O_{11}$ series the structure of which was studied on a single crystal was $Ho_4Mo_4O_{11}$.[5] The intensity data collections for the crystals of the other members investigated in the present study were carried out on a Nonius CAD-4 diffractometer equipped with graphite-monochromatized Mo Kα (λ = 0.71073 Å) radiation at 293 K. Accurate cell parameters were obtained by least-squares refinements of the setting angles of a set of 25 reflections in the 10−32° Θ range which was taken identical for all crystals studied. Three orientation and three intensity control reflections were checked every 250 reflections and every 1 h, respectively, and showed no significant variation over the data collection. Data were corrected for Lorentz−polarization using the MolEN package,[9] and an absorption correction based on the crystal shape[10] or on the Ψ scan method[11] was applied. Positional parameters of $Ho_4Mo_4O_{11}$ were used in the first stages of the refinements. The final refinement cycles included the atomic coordinates, anisotropic displacement parameters for all atoms. The structures were refined on F^2 by full-matrix least-squares methods with the SHELXL-97 program.[12] A refinement of the occupancy factors for the rare-earth sites in all crystals investigated confirmed that they are fully occupied. A summary of the experimental details and refinement procedures is presented in Table 1, and selected Mo−Mo and Mo−O interatomic distances are reported in Tables 2 and 3, respectively.

Electrical Resistivity Measurements. The ac resistivity was measured on single crystals at 80 Hz with current amplitudes in the range 0.5−6 μA using standard four-probe techniques between 300 and 80 K. Ohmic contacts were made by attaching molten indium ultrasonically.

Magnetic Susceptibility Measurements. Susceptibility data were collected on cold pressed powder samples (ca. 150 mg) in the temperature range between 1.8 and 300 K on a SHE-906 SQUID

(8) Ramanujachary, K. V.; Greenblatt, M.; Jones, E. B.; McCarroll, W. H. *J. Solid State Chem.* **1993**, *102*, 69.
(9) Fair, C. K. *MolEN, An Interactive Intelligent System for Crystal Structure Analysis*; Enraf-Nonius, Delft Instruments X-ray Diffraction BV: Rontgenweg 1, 2624 BD Delft, The Netherlands, 1990.
(10) De Meulenaar, J.; Tompa, H. *Acta Crystallogr., Sect. A* **1965**, *19*, 1014−1018.
(11) North, A. C. T.; Phillips, D. C.; Mathews, F. S. *Acta Crystallogr.* **1968**, *A24*, 351.
(12) Sheldrick, G. M. *SHELXL97, Program for the Refinement of Crystal Structures*; University of Göttingen: Göttingen, Germany, 1997.

Table 2. Selected Mo−Mo Distances (Å) for $R_4Mo_4O_{11}$ (R = Sm−Tm, Y)

		Sm	Eu	Gd	Tb	Dy	Ho	Er	Tm	Y
Mo(1)−Mo(1)	*a*	3.1190(5)	3.1115(5)	3.1051(7)	3.0929(6)	3.0842(9)	3.0763(9)	3.0685(7)	3.0593(7)	3.0756(5)
Mo(1)−Mo(1)	*f*	2.5988(5)	2.5927(5)	2.5891(7)	2.5835(6)	2.5798(9)	2.5750(9)	2.5711(7)	2.5689(7)	2.5761(6)
Mo(1)−Mo(2)	*e*	2.7458(4)	2.7450(4)	2.7428(6)	2.7422(5)	2.7414(7)	2.7391(7)	2.7375(6)	2.7367(5)	2.7407(5)
Mo(1)−Mo(2)	*d*	2.7844(4)	2.7826(4)	2.7802(6)	2.7735(5)	2.7745(7)	2.7716(7)	2.7690(6)	2.7663(5)	2.7714(5)
Mo(1)−Mo(3)	*c*	2.8148(4)	2.8146(4)	2.8118(5)	2.8081(5)	2.8067(7)	2.8037(7)	2.8019(6)	2.7996(5)	2.8037(5)
Mo(1)−Mo(3)	*b*	2.8251(4)	2.8230(4)	2.8196(5)	2.8138(5)	2.8122(7)	2.8094(6)	2.8060(5)	2.8032(5)	2.8083(5)
Mo(2)−Mo(2)	*g*	2.9104(7)	2.9103(7)	2.9089(10)	2.9067(9)	2.9098(12)	2.907(1)	2.907(1)	2.9043(9)	2.9098(9)
Mo(2)−Mo(3)	*h*	2.8634(1)	2.8565(1)	2.8515(1)	2.8425(1)	2.8363(1)	2.830(1)	2.8240(1)	2.8181(1)	2.8302(1)
Mo(3)−Mo(3)	*i*	2.5988(5)	2.5927(5)	2.5946(10)	2.5958(9)	2.599(1)	2.600(1)	2.602(1)	2.604(1)	2.5989(9)

Table 3. Selected Mo−O Distances (Å) for $R_4Mo_4O_{11}$ (R = Sm−Tm, Y)

	Sm	Eu	Gd	Tb	Dy	Ho	Er	Tm	Y
Mo(1)−O(4)	2.065(3)	2.064(2)	2.059(4)	2.061(3)	2.061(4)	2.057(4)	2.050(3)	2.051(3)	2.057(3)
Mo(1)−O(5)	2.081(2)	2.076(2)	2.072(3)	2.068(3)	2.070(5)	2.063(4)	2.064(3)	2.065(3)	2.067(2)
Mo(1)−O(1)	2.083(2)	2.082(2)	2.071(3)	2.075(3)	2.075(4)	2.070(4)	2.071(3)	2.067(3)	2.068(3)
Mo(1)−O(6)	2.086(2)	2.087(2)	2.086(3)	2.078(3)	2.078(4)	2.080(4)	2.080(3)	2.083(3)	2.077(2)
Mo(1)−O(7)	2.088(2)	2.089(2)	2.086(3)	2.079(2)	2.083(4)	2.080(4)	2.087(3)	2.083(3)	2.084(2)
Mo(2)−O(5)	2.066(3)	2.064(3)	2.068(4)	2.067(4)	2.062(6)	2.072(4)	2.069(4)	2.064(4)	2.072(4)
Mo(2)−O(4)	2.071(3)	2.070(3)	2.069(5)	2.068(4)	2.075(5)	2.073(6)	2.074(4)	2.069(4)	2.076(4)
Mo(2)−O(2) (×2)	2.089(2)	2.085(2)	2.087(3)	2.083(3)	2.080(4)	2.073(5)	2.077(3)	2.078(3)	2.084(3)
Mo(3)−O(6)	2.034(3)	2.035(3)	2.030(4)	2.025(4)	2.030(5)	2.019(5)	2.031(5)	2.034(4)	2.029(4)
Mo(3)−O(7)	2.059(3)	2.059(3)	2.054(4)	2.053(4)	2.048(6)	2.044(5)	2.050(4)	2.058(4)	2.049(4)
Mo(3)−O(2) (×2)	2.137(2)	2.133(2)	2.131(3)	2.129(3)	2.125(4)	2.117(4)	2.121(3)	2.114(3)	2.123(2)

magnetosusceptometer at applied fields ranging from 0.1 to 0.4 T. The data were subsequently corrected for the diamagnetic contribution of the sample holder.

Electronic Band Structure Calculations. Self-consistent ab initio band structure calculations were carried out on the crystal structure of $Y_4Mo_4O_{11}$ with the scalar relativistic tight binding linear muffin-tin orbital method in the atomic sphere approximation (TB-LMTO-ASA)[13] including the combined correction.[14] Exchange and correlation were treated in the local density approximation using the von Barth−Hedin local exchange correlation potential.[15] The Wigner−Seitz atomic sphere radii were determined using the automatic procedure.[14] The full LMTO basis set consisted of 5s, 5p, 4d, and 4f functions for Y and Mo spheres, 2s, 2p, and 3d functions for O spheres, and s, p, and d functions for "empty spheres". The eigenvalue problem was solved using the following minimal basis set obtained from the Löwdin downfolding technique:[16] Y 5s and 4d; Mo 5s, 5p, and 4d; O 2p; and interstitial s LMTOs. The *k* space integration was performed using the tetrahedron method.[17] Charge self-consistency and average properties were obtained from 84 irreducible *k* points.

Results and Discussion

Lattice Parameter Trends. We have summarized in Table 1 the lattice parameters of the $R_4Mo_4O_{11}$ compounds. Figure 1 shows a decrease in all lattice parameters and volumes of the orthorhombic unit cells as one moves through the series from the Nd to the Tm compound. These trends reflect the well-known lanthanide contraction and indicate that all rare earths are trivalent. The lattice parameters of the yttrium compounds are close to those of the holmium compounds, as is frequently observed in oxide systems.

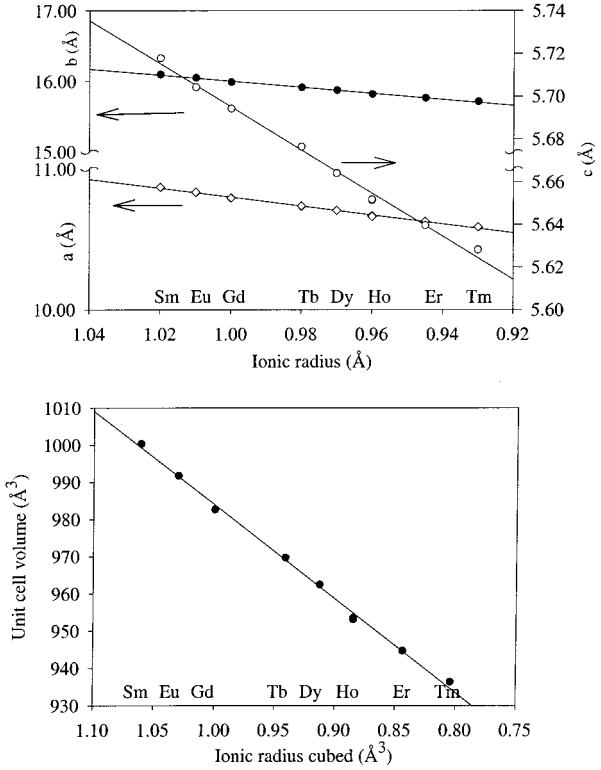

Figure 1. Variations of the lattice parameters of the orthorhombic $R_4Mo_4O_{11}$ members as a function of the crystal radius of the rare-earth cation.

Crystal Structures. The crystal structure of the $R_4Mo_4O_{11}$ compounds is dominated by Mo−Mo bondings manifested in infinite chains composed of edge-shared Mo_6 octahedral clusters with oxygen atoms above all free edges and corners (Figure 2). Thereby, the Mo atoms are coordinated to 11 atoms. The apical Mo1 atom is bonded to five Mo and five O atoms, and the two waist Mo2 and Mo3 atoms are bonded to seven Mo and four O atoms. The originality of the R_4-

(13) (a) Andersen, O. K. *Phys. Rev. B* **1975**, *12*, 3060. (b) Andersen, O. K.; Jepsen, O. *Phys. Rev. Lett.* **1984**, *53*, 2571. (c) Andersen, O. K.; Jepsen, O.; Glötzel, D. In *Highlights of condensed-matter theory*; Bassani, F., Fumi, F., Eds.; North-Holland: New York, 1985. (d) Lambrecht, W. R.; Andersen, O. K. *Phys. Rev. B* **1986**, *34*, 2439.
(14) Jepsen, O.; Andersen, O. K. *Z. Phys. B* **1995**, *97*, 35.
(15) Von Barth, U.; Hedin, L. *J. Phys. C* **1972**, *5*, 1629.
(16) Lambrecht, W. R.; Andersen, O. K. *Phys. Rev. B* **1986**, *34*, 2439.
(17) Blöchl, P. E.; Jepsen, O.; Andersen, O. K. *Phys. Rev. B* **1994**, *49*, 16223.

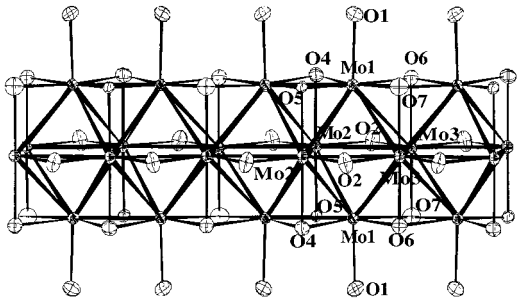

Figure 2. A section of one molybdenum oxide cluster chain. The repeat unit comprises two Mo_6 octahedra.

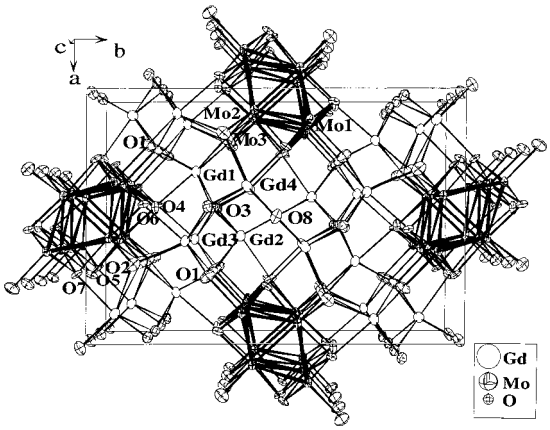

Figure 3. The crystal structure of $R_4Mo_4O_{11}$ as viewed down the *c* axis, parallel to the direction of the chain growth. Thick lines denote Mo−Mo bonding and thin lines, Mo−O and R−O bonding. Ellipsoids are drawn at the 97% probability level.

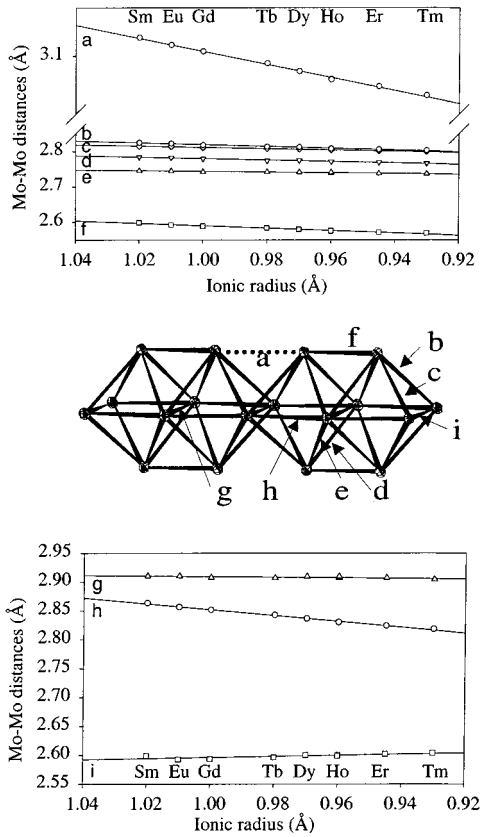

Figure 4. Variations of the Mo−Mo distances as a function of the crystal radius of the rare-earth cation.

Mo_4O_{11} compounds with respect to the other known infinite chain structures resides in the dilution of the chains with the rare-earth atoms (Figure 3). Indeed, in the previous compounds, the infinite metal chains are always connected through bridging oxygen atoms in, at least, one direction perpendicular to the chains. In this new compound, the Mo cluster chains do not share oxygen atoms since we always have the sequence Mo−O−R−O−Mo. Moreover, two crystallographically independent oxygen atoms O3 and O8 are not associated with the molybdenum oxygen network sublattice and are only bonded to R^{3+} cations.

Mo−Mo Bonds. The most striking feature within the Mo infinite chains is the pairwise distortion occurring between the apical molybdenum atoms Mo1, as shown in Figure 2. This pairing previously observed in $ZnMo_8O_{10}$[4] and $Gd_4Mo_{18}O_{32}$[6] is accompanied by alternating short and long bond distances between the molybdenum atoms of the common edges. The short Mo1−Mo1 bond distance between the apical molybdenum atoms ranges between 2.5982(7) Å in $Sm_4Mo_4O_{11}$ and 2.5687(9) Å in $Tm_4Mo_4O_{11}$ while the long one which is essentially nonbonding, decreasing from 3.1196(7) Å in $Sm_4Mo_4O_{11}$ to 3.0595(9) Å in $Tm_4Mo_4O_{11}$. The bond distance between the Mo atoms of the shared edge is shorter (Mo3−Mo3: 2.5988(5)−2.604(1) when going from the Sm to the Tm compound) when the apical−apical interaction is weaker, and longer (Mo2−Mo2: 2.9104(7)−2.9043(9)) when the interaction between the apex Mo atoms is stronger. This behavior was also observed in $ZnMo_8O_{10}$[4] and $Gd_4Mo_{18}O_{32}$.[6] The other Mo−Mo distances range between 2.738 and 2.863 Å (see Table 2). In Figure 4, we have plotted the different Mo−Mo distances as a function of the ionic radius of the rare earth. While the edge-shared distances Mo2−Mo2 and Mo3−Mo3 are quasi-constant (*g* and *i* in Figure 4) through the series, we can see that the remaining Mo−Mo distances decrease almost linearly when the ionic radius of the R^{3+} cation diminishes. The cationic charge transfer toward the metallic chains being identical in all compounds, it is clear that the latter trend results essentially from a sterical effect of the rare earth. The average of the Mo−Mo distances within the Mo_8O_{16} repeat unit is of the order of 2.80 Å, which differs little from that observed in the previous infinite chain compounds (e.g., 2.803 Å in $NaMo_4O_6$, 2.790 Å in $Mn_{1.5}Mo_8O_{10}$, 2.799 Å in $Sc_{0.75}Zn_{1.25}Mo_4O_7$, and 2.809 Å in $ZnMo_8O_{10}$).

Mo−O Bonds. The eight independent oxygen atoms can be divided into five distinct types according to their coordination geometries. Oxygen O1 is coordinated by one Mo atom and three rare-earth cations forming a distorted tetrahedron. Oxygen O2 is surrounded by two molybdenum atoms and three cations. O3 and O8 are only surrounded by four rare-earth cations in approximately tetrahedral symmetry. O4 and O5 are coordinated by three Mo and one rare earth in a sawhorse geometry. Finally, O6 and O7 are also bounded to three Mo and one rare earth in a very distorted tetrahedral geometry. The Mo−O distances range between 2.019 and 2.137 Å with average values of about 2.075 Å (Table 3).

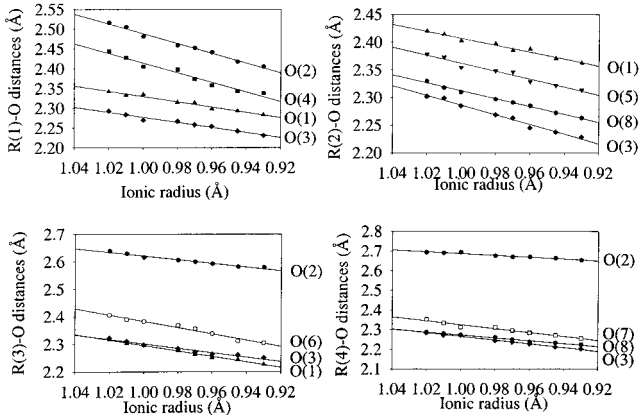

Figure 5. Variations of the R−O distances as a function of the crystal radius of the rare-earth cation.

Rare-Earth Environments. The environments of the four crystallographically inequivalent rare-earth cations consist of seven oxygen atoms placed at the vertexes of a distorted monocapped trigonal prism, the triangular faces being perpendicular to *c*. However, while, for the R1 and R2 sites, the seven R−O distances are uniformly distributed in the domain 2.24−2.52 Å, we observe five short R−O distances in the 2.21−2.41 Å range and two larger ones of about 2.65 Å for the R3 and R4 sites. In agreement with the lanthanide contraction, all the R−O distances decrease quasi-continuously with increasing atomic number as shown in Figure 5. The shortest distance between rare-earth atoms occurs between R3 and R4 and is in the range 3.35−3.37 Å when going from the samarium to the thulium.

Bond-Length Bond-Strength Formula. The estimation of the oxidation states of molybdenum and, consequently, of the number of electrons per Mo_4 fragment could be performed on these compounds using the empirical bond length-bond strength relationship developed by Brown and Wu[18] for Mo−O bonds:

$$s(\mathrm{Mo-O}) = [d(\mathrm{Mo-O})/1.882]^{-6}$$

In the above formula, *s*(Mo−O) is the bond strength in valence units, *d*(Mo−O) is the observed Mo−O bond distance in Å, 1.882 Å corresponds to a Mo−O single bond distance, and the exponential parameter −6 is characteristic of the Mo atom. For the nine compounds whose the crystal structures were determined in this work, these calculations lead to values in the range 13.9(1)−14.1(1) e^- per Mo_4, respectively, which are in good agreement with the value of 14 e^- based on the stoichiometry.

Electronic Study. As we have seen, the infinite chains in the $R_4Mo_4O_{11}$ compounds are highly distorted compared to those in the $NaMo_4O_6$ compound. EHT calculations made on the undistorted chain by Hughbanks and Hoffmann indicate that distortions are expected for MCE greater than 13 e^-.[19] In Figure 6, we have depicted the three types of distortion observed for the trans-edge-shared Mo_6 infinite chain to date. The first one, which is the more simple and is

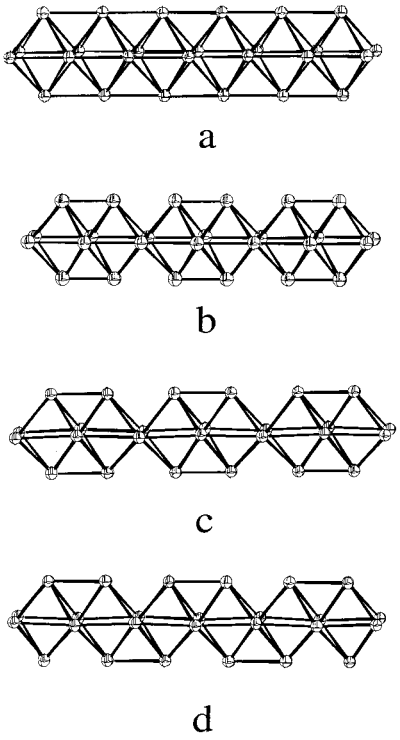

Figure 6. The undistorted infinite chains of trans-edge-sharing Mo_6 octahedra in $NaMo_4O_6$ (a) and the three type types of distortion observed to date in $R_4Mo_4O_{11}$ (b), $ZnMo_8O_{10}$ (c), and $Sc_{0.75}Zn_{1.25}Mo_4O_7$ (d).

observed in the present compounds, results from a symmetrical pairing of the apical Mo with respect to the basal plane accompanied by a long short pattern of the Mo−Mo distances of the shared edges. The second type of distortion is similar to the first one with in addition a slight tilting of the basal plane with a dihedral angle of about 173°. It occurs in $ZnMo_8O_{10}$ (MCE = 15 e^-), for example. The third one results from a tilting of the Mo_6 octahedra and leads to an antisymmetrical pairing of the apical Mo atoms as found in $Sc_{0.75}Zn_{1.25}Mo_4O_7$ (MCE = 14.75 e^-). EHT calculations performed by Hughbanks and Hoffmann on the latter compound allowed them to show that, because of the occupation of antibonding bands, systems with an electron count greater than 13 MCE per Mo_4 repeat unit should distort. The main effect on the band structure is the apparition of a small band gap for 14 MCE separating occupied bonding bands from vacant antibonding ones. This arises because of the loss of the basal symmetric plane of the chain. In fact two crossing bands built up from $x^2 - y^2$ apical Mo atoms and lying around the Fermi level in the regular chain can mix. This results in an avoided crossing of these bands and the opening of a small band gap.[19] Because of the presence of 14 MCE per Mo_4 repeat unit in the $R_4Mo_4O_{11}$ compounds, a distortion of the chain can therefore be envisioned. Considering the strong similarity of the two distortions (called "tilting" for the one observed in $Sc_{0.75}Zn_{1.25}Mo_4O_7$ and "pairing" in $R_4Mo_4O_{11}$ compounds), an effect on the electronic structure of the same kind can be foreseen. A density of states curve computed for $Y_4Mo_4O_{11}$ using density functional calculations is shown in Figure 7. A small gap of about 0.1 eV separates the occupied band from the vacant

(18) Brown, I. D.; Wu, K. K. *Acta Crystallogr.* **1976**, *B32*, 1957.
(19) Hughbanks, T.; Hoffmann, R. *J. Am. Chem. Soc.* **1983**, *105*, 3528.

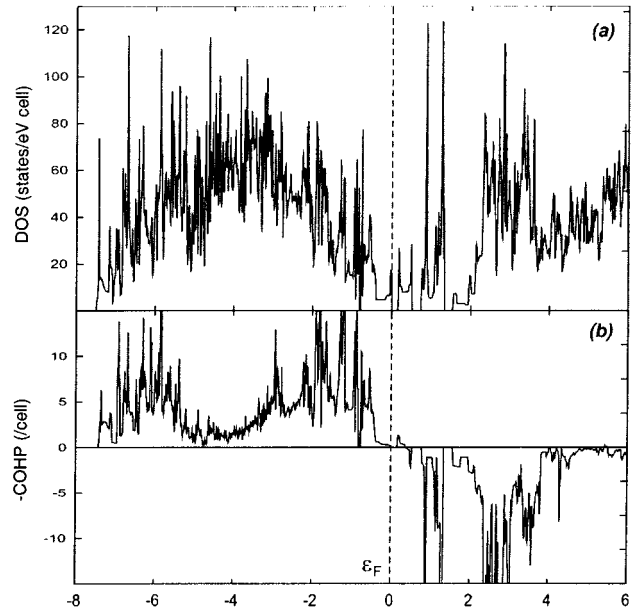

Figure 7. DFT calculations for $Y_4Mo_4O_{11}$: (a) total DOS and (b) COHP for Mo−Mo bonds ranging from 2.576 to 3.076 Å.

ones. A crystal orbital Hamiltonian population (COHP) curve indicates that all occupied bands are Mo−Mo bonding. No significant bonding occurs in long Mo1−Mo1 contacts as shown by the integrated COHP value of −0.07 eV; this value can be compared to the one for the averaged Mo−Mo integrated COHP equal to −1.25 eV. Thus, as for the "tilting" distortion in $Sc_{0.75}Zn_{1.25}Mo_4O_7$, the "pairing" distortion stabilizes the structure. Wheeler and Hoffmann studied the electronic structure of trans-edge-sharing octahedral clusters Mo_{18} and Mo_{22} where the pairing distortion is present.[20] They showed that the $x^2 - y^2$ bands are driving the distortion and also that the pairing of apical molybdenum atoms along the chain and basal Mo−Mo bonding perpendicular to the chain are electronically coupled. This explains the shorter Mo3−Mo3 and longer Mo2−Mo2 distances observed in $R_4Mo_4O_{11}$ compounds. The integrated COHP of −2.49 eV indicates a strong bond between Mo3−Mo3 atoms compared to the averaged Mo−Mo integrated COHP value of −1.25 eV.

Electrical Properties. Four probe electrical resistivity measurements carried out on single crystals of $Y_4Mo_4O_{11}$, $Dy_4Mo_4O_{11}$, $Er_4Mo_4O_{11}$, and $Tm_4Mo_4O_{11}$ indicate that these materials are semiconducting. Plots of log ρ vs 1000/T for all four crystals measured are shown in Figure 8. A narrow band gap of the order of 0.05 eV was calculated. The room-temperature resistivities of the single crystals measured along the c axis (direction of the chain growth) range from 0.2 to 0.9 Ω·cm, while the resistivities in the (a,b) plane are about 1000 times greater. No temperature dependence of the electrical resistivity was recorded in the latter configuration at lower temperature because the sample resistance was beyond the detection limit of our instrumentation. This semiconducting property agrees with the theoretical results since a small band gap of about 0.1 eV is computed for $Y_4Mo_4O_{11}$ (see Figure 7).

(20) Wheeler, R. A.; Hoffmann, R. *J. Am. Chem. Soc.* **1988**, *110*, 7315.

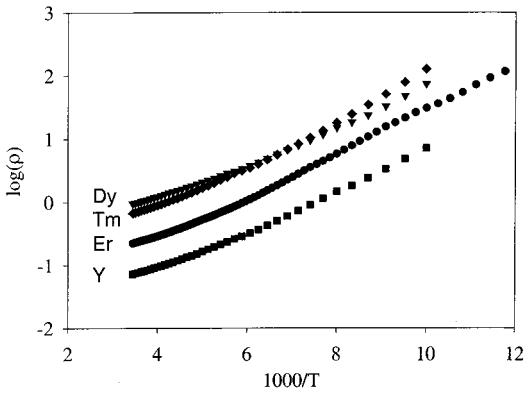

Figure 8. Arrhenius plots for the $R_4Mo_4O_{11}$ compounds.

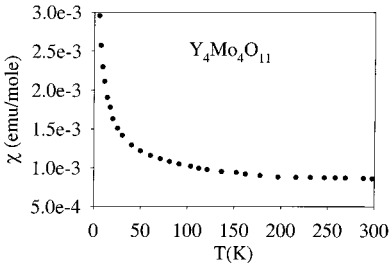

Figure 9. Temperature dependence of the susceptibility for $Y_4Mo_4O_{11}$.

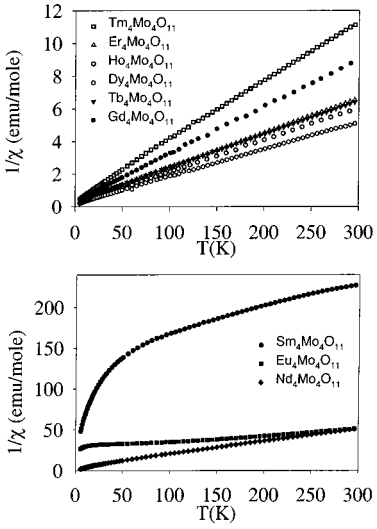

Figure 10. Reciprocal susceptibilities of the compounds $R_4Mo_4O_{11}$ (R = Nd, Sm, Eu, Gd, Tb, Dy, Ho, Er, and Tm) as a function of temperature.

Magnetic Properties. $Y_4Mo_4O_{11}$. The magnetic susceptibility study of $Y_4Mo_4O_{11}$ indicates a temperature independent behavior in the range 100−300 K with a $\chi_{RT} = 8.6\ 10^{-4}$ emu/mol (Figure 9) consistent with the absence of localized moments on the Mo chains. The low-temperature paramagnetic tail arises probably from impurities in the starting materials.

$R_4Mo_4O_{11}$ with R = Nd, Sm, Eu, Gd, Tb, Dy, Ho, Er, and Tm. The magnetic behavior of these compounds is dominated by the magnetism of the rare earth. The variations of the inverse susceptibilities as a function of the temperature for the $R_4Mo_4O_{11}$ compounds with magnetic rare earths are displayed in Figure 10. It can be seen from these plots that, with the exception of $Sm_4Mo_4O_{11}$ and $Eu_4Mo_4O_{11}$, which

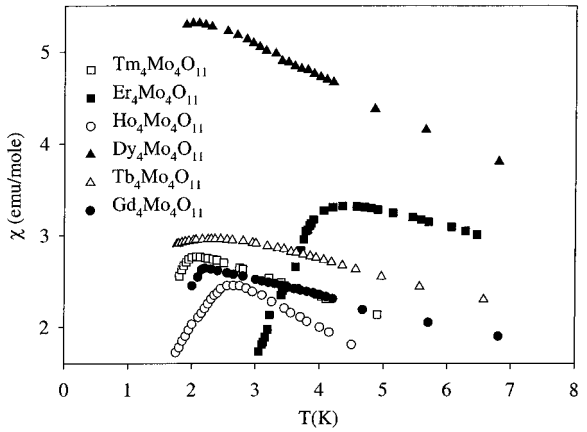

Figure 11. Temperature dependences of the susceptibilities of the compounds $R_4Mo_4O_{11}$ (R = Gd, Tb, Dy, Ho, Er, and Tm) below 7 K.

Table 4. Magnetic Susceptibility Data for the $R_4Mo_4O_{11}$ (R = Sm, Eu, Gd, Tb, Dy, Ho, Er, Tm, and Y) Compounds

compound	μ_B/R^{3+}	$\mu_{B_{th}}$	θ_p (K)	T_N (K)	fit region
$Y_4Mo_4O_{11}$	0	0			
$Nd_4Mo_4O_{11}$	3.61	3.62	−35.6		80−300
$Sm_4Mo_4O_{11}$	1.26	0.84	−131.8		100−300
$Eu_4Mo_4O_{11}$	4.7	0.00	−264.5		180−300
$Gd_4Mo_4O_{11}$	7.92	7.94	−10.7	2.15	20−300
$Tb_4Mo_4O_{11}$	9.61	9.72	−18.7	2.30	100−300
$Dy_4Mo_4O_{11}$	10.68	10.63	−10.7	2.05	20−300
$Ho_4Mo_4O_{11}$	10.05	10.60	−7.1	2.60	
$Er_4Mo_4O_{11}$	9.75	9.59	−15.2	4.35	100−300
$Tm_4Mo_4O_{11}$	7.50	7.57	−18.6	2.07	100−300

show Van Vleck paramagnetism, all compounds follow a Curie−Weiss law $\chi = C/(T - \Theta)$ above 100 K. The magnetic moments calculated from the slopes of the linear regions of the plots and the Weiss constants Θ are given in Table 4 and compare well with those expected for free ions R^{3+}. In addition, the $R_4Mo_4O_{11}$ compounds, with R = Gd−Tm, show maxima of susceptibility between 2.05 and 4.35 K (see Table 4 and Figure 11) that can be attributed to antiferromagnetic ordering transitions. This assumption has been confirmed for $Ho_4Mo_4O_{11}$ by neutron diffraction where additional magnetic peaks were observed below 2.6 K (Figure 12). The study of the magnetic structures of the $R_4Mo_4O_{11}$ (R = Tb, Dy, Ho, Er, Tm) compounds will be published elsewhere. For the $Sm_4Mo_4O_{11}$ compound, the experimental effective magnetic moment at room temperature $\mu_{exp} = 1.48\ \mu_B/Sm^{3+}$ determined from the formula $\mu_{exp} = 2.83[(\chi_{cgs}/4)T]^{1/2}\ \mu_B/Sm^{3+}$ correlates well the value of 1.55 μ_B calculated by Van Vleck for Sm^{3+} at 293 K with a screening value $\sigma = 33$ as well with the experimental values that range between 1.32 and 1.63.[21]

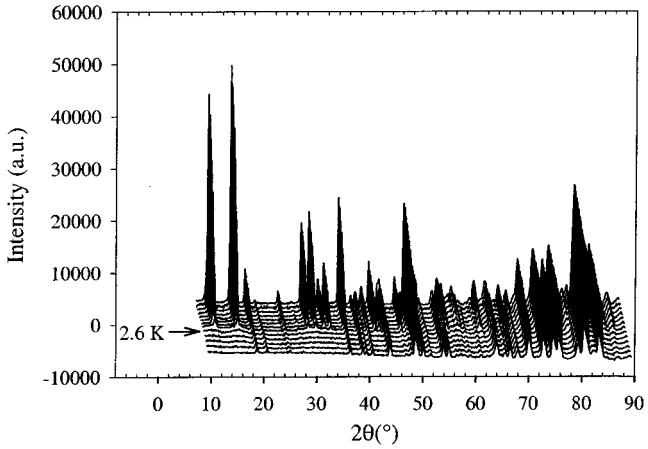

Figure 12. Temperature dependence of the neutron powder pattern (λ = 2.426 Å) of $Ho_4Mo_4O_{11}$ between 5 and 1.4 K.

Regarding the $Eu_4Mo_4O_{11}$ compound, the experimental value of 3.8 μ_B/Eu^{3+} found is slightly higher that the expected value of 3.5 μ_B/Eu^{3+} at room tempetature.[21] This arises from the presence of a small amount of $EuMo_5O_8$ that contains divalent europium ($\mu_{exp} = 7.94\ \mu_B/Eu^{2+}$).

In summary, compounds isostructural with $Ho_4Mo_4O_{11}$, which was first described in 1991 by Gall et al.,[6] have been synthesized with rare-earth elements going from neodymium to thulium. Electrical and magnetic properties have been investigated for the whole family of compounds. The resistivity measurements show that the $R_4Mo_4O_{11}$ compounds exhibit semiconducting behavior with a small activation energy of about 0.05 eV at high temperature. Magnetic data reveal paramagnetism of the trivalent rare-earth cations. The members with R = Gd−Tm also undergo antiferromagnetic transition in the 2.05−4.05 K temperature range. Theoretical calculations show that the pairing distortion stabilizes the structure for the experimental electron count. A further step in this study would be to substitute some of the trivalent rare earths by a divalent cation such as Ca^{2+} for lowering the MCE and thus may be rendering these compounds metallic.

Acknowledgment. We thank Dr. H. Noël for the collection of the magnetic susceptibility data.

Supporting Information Available: X-ray crystallographic files for the $R_4Mo_4O_{11}$ (R = Y, Nd, Sm−Tm) compounds, in CIF format. This material is available free of charge via the Internet at http://pubs.acs.org.

IC011000I

(21) Van Vleck, J. H. *The Theory of Electric and Magnetic Susceptibilities*; Oxford University Press: London, 1965.